Journal of Magnetism and Magnetic Materials 481 (2019) 100–103

Contents lists available at ScienceDirect

Journal of Magnetism and Magnetic Materials

journal homepage: www.elsevier.com/locate/jmmm

Research articles

# The decisive role of magnetic anisotropy in honeycomb layered $Li_3Ni_2SbO_6$ and $Na_3Ni_2SbO_6$

J. Werner[a,*], W. Hergett[a], J. Park[a], C. Koo[a], E.A. Zvereva[b], A.N. Vasiliev[b,c,d], R. Klingeler[a,e]

[a] Kirchhoff Institute of Physics, Heidelberg University, INF 227, D-69120 Heidelberg, Germany
[b] Faculty of Physics, Moscow State University, Moscow 119991, Russia
[c] National University of Science and Technology (MISiS), Moscow 119049, Russia
[d] Russia National Research, South Ural State University, Chelyabinsk 454080, Russia
[e] Centre for Advanced Materials, Heidelberg University, INF 225, D-69120 Heidelberg, Germany

ARTICLE INFO

*Keywords:*
Honeycomb layers
Magnetisation
Magnetism
Anisotropy
Phase diagram
Electron spin resonance

ABSTRACT

The decisive role of magnetic anisotropy even in systems with small anisotropy is illustrated for the honeycomb-layered antiferromagnets $A_3Ni_2SbO_6$ with $A$ = Li and Na. Both systems evolve long range magnetic order below $T_N$ = 14 and 16.5 K, respectively. The magnetic phase diagrams obtained from static magnetisation studies up to 15 T imply competing antiferromagnetic phases and a tricritical point at $T_N$. The phase boundaries are visible in the dynamic response of the antiferromagnetic resonance modes, too, which investigation by means of high frequency/high field electron spin resonance enables precise determination of magnetic anisotropy. The anisotropy gap amounts to $\Delta = 360 \pm 2$ GHz in $Na_3Ni_2SbO_6$ while in $Li_3Ni_2SbO_6$ orthorhombicity is associated with $\Delta = 198 \pm 4$ and $218 \pm 4$ GHz. Above $T_N$, the data imply short-range antiferromagnetic order up to at least 80 K. The data suggest a crucial role of anisotropy for selecting the actual spin structure at $B = 0$ T.

## 1. Introduction

Spin systems realised on layered honeycomb lattices exhibit a variety of quantum ground states which nature is determined by nearest and next nearest neighbour magnetic interactions. The resulting ground states may be, e.g., Néel-, zigzag-, stripe-, and different spiral-type or show spin gaps [1–5]. While geometric frustration may further affect the ground state spin configuration including the complete suppression of long-range magnetic order, also the spin size is crucial: while in the spin-1/2 case the particular spiral ground state [6,7] can be selected by quantum fluctuations, the spin-3/2 system can show robust nematic order [8]. Magnetic anisotropy may also play a decisive role. [6,9] Honeycomb lattices of $A_3Ni_2SbO_6$ hosting $Ni^{2+}$-ions with $S = 1$ provide further insight into this class of layered spin systems. Here, we present the magnetic phase diagrams obtained from static magnetisation, specific heat, and thermal expansion studies up to 15 T as well as investigations of the antiferromagnetic (AFM) resonance modes by means of high frequency/high field electron spin resonance. Our analysis of the data shows that magnetocrystalline anisotropy can play a decisive role in determining the magnetic properties of the materials.

## 2. Experiment

Polycrystalline $A_3Ni_2SbO_6$ was prepared by conventional solid state synthesis as reported previously [10]. For the measurements the sample was pressed into a pellet with an diameter of ~ 3 mm. Magnetisation in static magnetic fields up to 5 T was studied by means of a Quantum Design MPMS-XL5 SQUID magnetometer and in fields up to 15 T in a home-built vibrating sample magnetometer (VSM) [11]. HF-ESR measurements were performed on a pressed pellet of the material by means of a phase-sensitive millimetre-wave vector network analyser (MVNA) from AB Millimetré covering the frequency range from 30 to 1000 GHz and in magnetic fields up to 16 T. [12].

## 3. Results and discussion

The magnetic field effect on both the static magnetic susceptibility $\chi = M/B$ and its derivative $\partial(\chi T)/\partial T$, in the vicinity of $T_N$ , is shown in Fig. 1. Fisher's specific heat $\partial(\chi T)/\partial T$ [13] derived from $\chi(B = 1$ T) shows a sharp anomaly indicating the onset of long-range antiferromagnetic order at $T_N$ = 14 K. This agrees to the Néel temperature $T_N(B = 0$ T) = 14.2(5) K as determined by neutron diffraction [14]. Upon application of $B \geqslant 1$ T, the anomaly broadens and covers a regime

* Corresponding author.
*E-mail address:* Johannes.Werner@kip.uni-heidelberg.de (J. Werner).

https://doi.org/10.1016/j.jmmm.2019.02.054
Received 26 July 2018; Received in revised form 6 February 2019; Accepted 18 February 2019
Available online 19 February 2019
0304-8853/ © 2019 Elsevier B.V. All rights reserved.

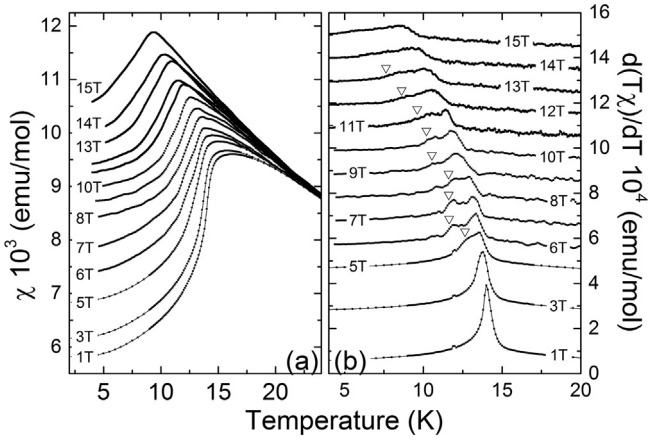



**Fig. 1.** (a) Static susceptibility $\chi = M/B$ of $Li_3Ni_2SbO_6$ and (b) the derivative $\partial(\chi T)/\partial T$ vs. temperature in external magnetic fields ranging from 1 to 15 T.

of, depending on $B$, 1.5–4 K. At high magnetic fields, only a step is observed at the high temperature edge of the anomaly, which signals $T_N$ ($B$). It has been shown by comparing thermal expansion and magnetisation data on $Na_3Ni_2SbO_6$ that broadening of the anomaly is associated with the presence of a transition between two antiferromagnetic phases. To be specific, a shoulder, or rather a second peak, develops at the low temperature edge of the anomaly for fields $\leqslant$ 5 T as indicated by open triangles in Fig. 1.

The presence of a phase boundary between two antiferromagnetic phases is evident when the magnetic susceptibility $\partial M(B)/\partial B$, at $T = 6$ K, is considered (see Fig. 2). The data, at 6 K, suggest three different phases separated by phase transitions at $B_{C1} \approx 6.7$ T and $B_{C2} \approx 13.9$ T, marked by black triangles. The anomaly at $B_{C1}$ appears as a broad peak in $\partial M/\partial B$. In contrast, $B_{C2}$ is associated with a kink in the magnetic susceptibility. At $T = 4.2$ K, $B_{C2}$ is above the field range accessible by our experiment. Upon moderate heating, $B_{C1}$ is only slightly affected while $B_{C2}$ is considerably suppressed. Though the anomalies are much broader at high magnetic field, the magnetic susceptibility is reminiscent to the one of $Na_3Ni_2SbO_6$ (Fig. 2b). The magnetisation data enable constructing the magnetic phase diagram in Fig. 3a. There are three antiferromagnetic phases which are separated by the phase boundaries $B_{C1}$ ($T$) and $B_{C2}$ ($T$). As shown above, there is only one distinct anomaly at $B = 1$ T which suggests tricritical points at finite magnetic field as shown in Fig. 3a. Please note larger error bars associated with the anomalies at 2 T$\leqslant B\leqslant$ 6 T which is indicated by the dashed phase boundaries.

The phase diagram presented in Fig. 3a significantly differs from the recently published one on the same compound in Ref. [16]. It also differs from the related material $Na_3Ni_2SbO_6$ (see Fig. 3b) where the AF2 phase extends to $B = 0$ T, yielding a tricritical point at $T_N$ [15]. While, the upper critical fields $B_{sat}$ indicating complete suppression of antiferromagnetic spin order is similar in both compounds. This implies similar antiferromagnetic exchange interactions which is corroborated by previously published DFT calculations as well as similar Weiss temperatures. [16].

The spin configuration in the AF1 ground state of $Li_3Ni_2SbO_6$ comprises zigzag ferromagnetic chains coupled antiferromagnetically in the plane and ferromagnetically along the $c$-direction. [14] Further insight is obtained from antiferromagnetic resonance (AFMR) studies by means of HF-ESR as, in the long-range spin ordered phase, HF-ESR is susceptible to the $q = 0$ magnon modes. The magnetic field dependence of the AFMR resonance frequency of $A_3Ni_2SbO_6$ is shown in Fig. 4. The AF1 spin configuration can be described by means of a two-sublattice mean field model [14] with uniaxial anisotropy. Fitting the resonances by such model gives the solid lines in Fig. 4. Our analysis yields the anisotropy gaps $\Delta = 360 \pm 2$ GHz in $Na_3Ni_2SbO_6$ as well as $\Delta = 198 \pm 4$ and $218 \pm 4$ GHz in $Li_3Ni_2SbO_6$. From $\Delta^2 \approx 2\gamma^2 B_E B_A \approx 2\gamma^2 B_{Sat} B_A$, with the exchange field $B_E$ and the anisotropy field $B_A$, we obtain $B_A = 1.1$ and 1.4 T in $Li_3Ni_2SbO_6$ and 2.9 T in $Na_3Ni_2SbO_6$. Anisotropy in $Na_3Ni_2SbO_6$ is more than two times stronger than in $Li_3Ni_2SbO_6$ which agrees to the observed values of $B_{C1}$ in both systems (see Fig. 3).

## 4. Conclusions

On the first glance, magnetic phase diagrams in $A_3Ni_2SbO_6$ ($A$ = Li, Na) seem to be very similar which is consistent to nearly identical magnetic exchange interactions found by DFT calculations on both systems [16]. However, as shown in Fig. 3, the phase boundaries are clearly different around $T_N$. This difference might originate from a different nature of the AF2 phases in both materials. In $Na_3Ni_2SbO_6$, AF2 is not a spin-flop phase as can be seen from the significant difference of $B_{C1}$ and the expected spin-flop field. In addition, there are pronounced structural changes and a sign change of the magnetostriction coefficient at $B_{C1}$ which further exclude a bare spin-flop scenario [15]. In contrast, $B_{C1}$ of $Li_3Ni_2SbO_6$ agrees to the spin flop field expected from analysing the ESR phase diagram. Furthermore, the resonance branch $\omega_3$ is well described in terms of the spin-flop mode (see Fig. 4a). We also note, that the phase boundary $B_{C1}$ ($T$) shows very small slope for $Li_3Ni_2SbO_6$ which is typical of a spin-flop transition while in $Na_3Ni_2SbO_6$ there is a strong temperature dependence yielding a tricritical point at $T_N$. In $Li_3Ni_2SbO_6$, in the vicinity of $T_N$ , i.e., at $T = 14$ K, $B = 3$ T is required to

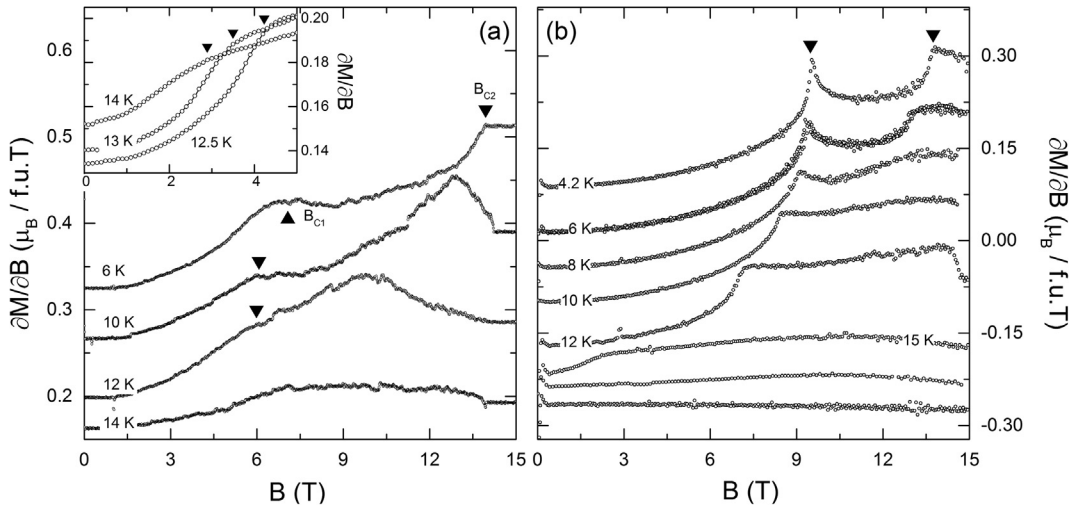



**Fig. 2.** Magnetic susceptibility $\partial M/\partial B$ as a function of the external magnetic field at constant temperatures for (a) $Li_3Ni_2SbO_6$ and (b) $Na_3Ni_2SbO_6$. [15].

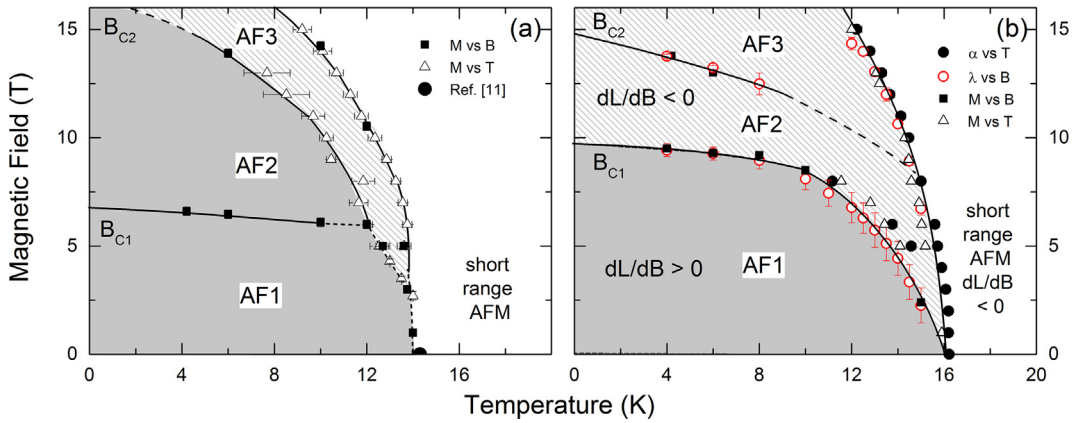



**Fig. 3.** Magnetic phase diagram of (a) $Li_3Ni_2SbO_6$ und (b) $Na_3Ni_2SbO_6$ [15]. The solid and dashed lines are guide to the eye. The Néel temperature $T_N$ ($B$ = 0 T) = 14.2(5) K of $Li_3Ni_2SbO_6$ was determined by neutron diffraction [14].

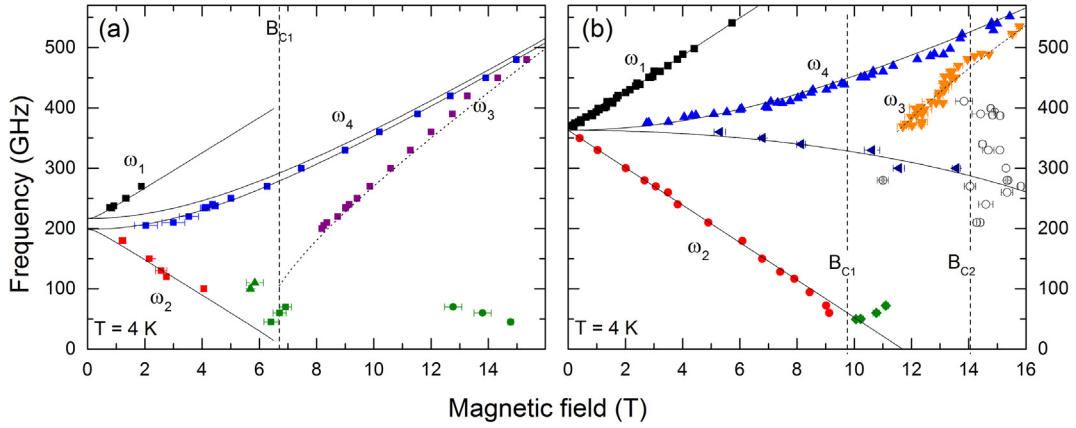



**Fig. 4.** Resonance frequencies of (a) $Li_3Ni_2SbO_6$ [14] and (b) $Na_3Ni_2SbO_6$ [15] vs. magnetic field. Solid lines represent fits of a two-sublattice AFM resonance model and dashed lines represent the high field $\omega_3$ resonance branch.

stabilize the AF3 phase (not AF2). We conclude that, in $Na_3Ni_2SbO_6$, there are nearly degenerated spin configurations AF1 and AF2 at $T_N$ while there is a more conventional spin-flop-like phase in $Li_3Ni_2SbO_6$ which is energetically well separated from AF1.

In summary, we have presented the phase diagrams of the quasi-two dimensional honeycomb-layered $A_3Ni_2SbO_6$ ($A$ = Li,Na). While both systems evolve long range magnetic order, $Na_3Ni_2SbO_6$ shows a tricritical point at $T_N$ and the field-induced AF2 phase is not a bare spin-flop phase. Smaller anisotropy, i.e., $B_A$ = 1.1 and 1.4 T as compared to 2.9 T, somehow counter-intuitively results in a rather typical spin-flop-like phase AF2 in $Li_3Ni_2SbO_6$. We conclude a crucial role of anisotropy for selecting the actual spin structure at $B$ = 0 T and for the competition of the three spin ordered phases.

## Acknowledgements

The authors thank A.U.B. Wolter for valuable support, and V.B. Nalbandyan for providing the samples for this study. J.W. acknowledges support from the HGSFP and IMPRS-QD. Partial support by the DFG via Project KL 1824/13 is gratefully acknowledged. A.N.V. acknowledges support from Russian Foundation for Basic Research Grant No. 18-502-12022. This work was supported by the Ministry of Education and Science of the Russian Federation in the framework of Increase Competitiveness Program of NUST (MISiS) Grant No. K2-2017-084, by act 211 of the government of the Russian Federation, Contracts No. 02.A03.21.0004 and 02.A03.21.0011.

## References

[1] P.H.Y. Li, R.F. Bishop, D.J.J. Farnell, C.E. Campbell, Phase diagram of a frustrated heisenberg antiferromagnet on the honeycomb lattice: the $J_1$-$J_2$-$J_3$ model, Phys. Rev. B 86 (2012) 144404, https://doi.org/10.1103/PhysRevB.86.144404.

[2] D.C. Cabra, C.A. Lamas, H.D. Rosales, Quantum disordered phase on the frustrated honeycomb lattice, Phys. Rev. B 83 (2011) 094506, https://doi.org/10.1103/PhysRevB.83.094506.

[3] E.A. Zvereva, O.A. Savelieva, Y.D. Titov, M.A. Evstigneeva, V.B. Nalbandyan, C.N. Kao, J.-Y. Lin, I.A. Presniakov, A.V. Sobolev, S.A. Ibragimov, M. Abdel-Hafiez, Y. Krupskaya, C. Jähne, G. Tan, R. Klingeler, B. Büchner, A.N. Vasiliev, A new layered triangular antiferromagnet $Li_4FeSbO_6$: spin order, field-induced transitions and anomalous critical behavior, Dalton Trans. 42 (2013) 1550–1566, https://doi.org/10.1039/C2DT31938A.

[4] J. Fouet, P. Sindzingre, C. Lhuillier, An investigation of the quantum $J_1 - J_2 - J_3$ model on the honeycomb lattice, Eur. Phys. J. B Cond. Matter Complex Syst. 20 (2) (2001) 241–254, https://doi.org/10.1007/s100510170273.

[5] C. Koo, E.A. Zvereva, I.L. Shukaev, M. Richter, M.I. Stratan, A.N. Vasiliev, V.B. Nalbandyan, R. Klingeler, Static and dynamic magnetic response of fragmented haldane-like spin chains in layered $Li_3Cu_2SbO_6$, J. Phys. Soc. Jpn. 85 (8) (2016) 084702, https://doi.org/10.7566/JPSJ.85.084702.

[6] S. Okubo, H. Wada, H. Ohta, T. Tomita, M. Fujisawa, T. Sakurai, E. Ohmichi, H. Kikuchi, Anomalous spin dynamics observed by high-frequency esr in honeycomb lattice antiferromagnet $InCu_{2/3}V_{1/3}O_3$, J. Phys. Soc. Jpn. 80 (2) (2011) 023705, https://doi.org/10.1143/JPSJ.80.023705.

[7] M. Yehia, E. Vavilova, A. Möller, T. Taetz, U. Löw, R. Klingeler, V. Kataev, B. Büchner, Finite-size effects and magnetic order in the spin-$\frac{1}{2}$ honeycomb-lattice compound $InCu_{2/3}V_{1/3}O_3$, Phys. Rev. B 81 (2010) 060414, https://doi.org/10.1103/PhysRevB.81.060414.

[8] A. Mulder, R. Ganesh, L. Capriotti, A. Paramekanti, Spiral order by disorder and lattice nematic order in a frustrated heisenberg antiferromagnet on the honeycomb lattice, Phys. Rev. B 81 (2010) 214419, https://doi.org/10.1103/PhysRevB.81.214419.

[9] J. Werner, C. Koo, R. Klingeler, A.N. Vasiliev, Y.A. Ovchenkov, A.S. Polovkova, G.V. Raganyan, E.A. Zvereva, Magnetic anisotropy and the phase diagram of chiral $MnSb_2O_6$, Phys. Rev. B 94 (2016) 104408, https://doi.org/10.1103/PhysRevB.94.

104408.
[10] E.A. Zvereva, M.A. Evstigneeva, V.B. Nalbandyan, O.A. Savelieva, S.A. Ibragimov, O.S. Volkova, L.I. Medvedeva, A.N. Vasiliev, R. Klingeler, B. Buechner, Monoclinic honeycomb-layered compound $Li_3Ni_2SbO_6$: preparation, crystal structure and magnetic properties, Dalton Trans. 41 (2012) 572–580, https://doi.org/10.1039/C1DT11322D.
[11] R. Klingeler, B. Büchner, K.-Y. Choi, V. Kataev, U. Ammerahl, A. Revcolevschi, J. Schnack, Magnetism of hole-doped $CuO_2$ spin chains in $Sr_{14}Cu_{24}O_{41}$: experimental and numerical results, Phys. Rev. B 73 (2006) 014426, https://doi.org/10.1103/PhysRevB.73.014426.
[12] P. Comba, M. Grohauser, R. Klingeler, C. Koo, Y. Lan, D. Müller, J. Park, A. Powell, M.J. Riley, H. Wadepohl, Magnetic interactions in a series of homodinuclear lanthanide complexes, Inorgan. Chem. 54 (23) (2015) 11247–11258, https://doi.org/10.1021/acs.inorgchem.5b01673 pMID: 26588004.
[13] M.E. Fisher, Relation between the specific heat and susceptibility of an antiferromagnet, Philos. Mag.: J. Theor. Exp. Appl. Phys. 7 (82) (1962) 1731–1743, https://doi.org/10.1080/14786436208213705.
[14] A.I. Kurbakov, A.N. Korshunov, S.Y. Podchezertsev, A.L. Malyshev, M.A. Evstigneeva, F. Damay, J. Park, C. Koo, R. Klingeler, E.A. Zvereva, V.B. Nalbandyan, Zigzag spin structure in layered honeycomb $Li_3Ni_2SbO_6$: a combined diffraction and antiferromagnetic resonance study, Phys. Rev. B 96 (2017) 024417, https://doi.org/10.1103/PhysRevB.96.024417.
[15] J. Werner, W. Hergett, M. Gertig, J. Park, C. Koo, R. Klingeler, Anisotropy-governed competition of magnetic phases in the honeycomb quantum magnet $Na_3Ni_2SbO_6$ studied by dilatometry and high-frequency esr, Phys. Rev. B 95 (2017) 214414, https://doi.org/10.1103/PhysRevB.95.214414.
[16] E.A. Zvereva, M.I. Stratan, Y.A. Ovchenkov, V.B. Nalbandyan, J.-Y. Lin, E.L. Vavilova, M.F. Iakovleva, M. Abdel-Hafiez, A.V. Silhanek, X.-J. Chen, A. Stroppa, S. Picozzi, H.O. Jeschke, R. Valentí, A.N. Vasiliev, Zigzag antiferromagnetic quantum ground state in monoclinic honeycomb lattice antimonates $A_3Ni_2SbO_6$ (A = Li, Na), Phys. Rev. B 92 (2015) 144401, https://doi.org/10.1103/PhysRevB.92.144401.